Magnetic Hyperfine Interactions in the Mixed-Valence Compound $Fe_7(PO_4)_6$ from Mössbauer Experiments

Alexey V. Sobolev[1,*], Alena A. Akulenko[1], Iana S. Glazkova[1], Alexei A. Belik[2], Takao Furubayashi[3], Larisa V. Shvanskaya[1,4], Olga V. Dimitrova[1], Igor A. Presniakov[1]

[1]*Lomonosov Moscow State University, 119991 Moscow, Russia*

[2]*Research Center for Functional Materials, National Institute for Materials Science (NIMS), Namiki 1-1, Tsukuba, Ibaraki 305-0044, Japan*

[3]*Research Center for Magnetic and Spintronic Materials, National Institute for Materials Science (NIMS), Sengen 1-2-1, Tsukuba, Ibaraki 305-0047, Japan*

[4]*National University of Science and Technology "MISiS", 119049 Moscow, Russia*

[*]corresponding author, e-mail: *alex@radio.chem.msu.ru*, *salex12@rambler.ru*

Supporting Information

This section consists of a figure with results of magnetic measurements (curves *M* vs *H*) and also includes detailed information about the procedure of the calculation of a lattice contribution to the electric field gradient (EFG) tensor as well as crystal field calculations.

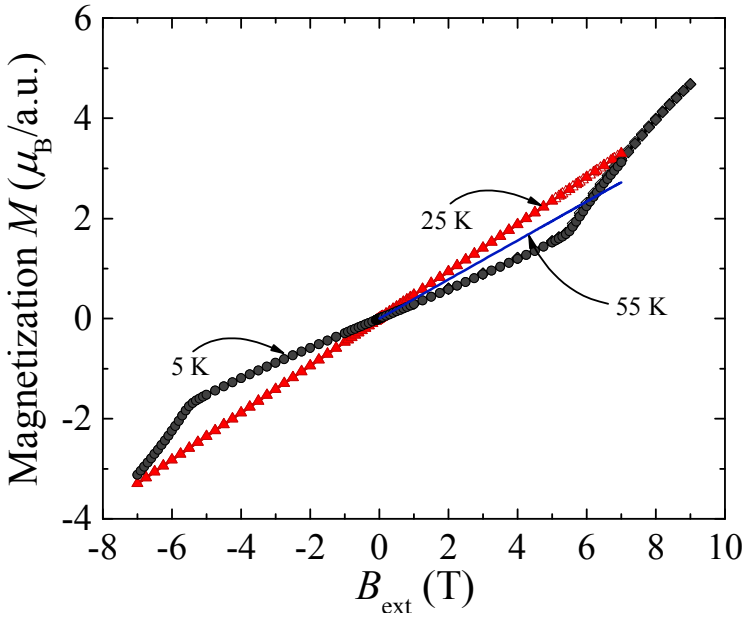

Figure S1. The field dependencies of magnetization *M* in $Fe_7(PO_4)_6$ measured at various temperatures.

1. ***Calculation of the "lattice" and the "overlap" contributions to the EFG.***

The lattice contribution to the EFG at the Fe^{3+} sites was calculated using a monopole-point-dipole model.[S1] The monopole contribution (V_{ij}^{mon}) is given by

$$V_{ij}^{\mathrm{mon}} = \sum_k Z_k (3x_{ik}x_{jk} - \delta_{ij} r_k^2)/r_k^5 , \qquad \text{(S1)}$$

where Z_k is the charge and x_{ik} (x_{jk}) are the Cartesian coordinates of the k-th ion with a distance r_k from the origin located at a given site, δ_{ij} is the Kronecher index. The dipole contribution V_{ij}^{dip} is

$$V_{ij}^{\mathrm{dip}} = \sum_k -3[(x_{ik}p_{ik})(5x_{ik}x_{jk} - \delta_{ij}r_k^2)/r_k^7 - (x_{ik}p_{ik} + x_{jk}p_{jk})/r_k^5], \qquad \text{(S2)}$$

where p_{ik} is the i-th component of the induced dipole moment on the k-th ion and the other symbols have the same meaning as in Eq. (S1). The components of the induced dipole moment are equal to

$$p_{ik} = \sum_i \alpha_{ij}^k E_j^k , \qquad \text{(S3)}$$

where α^k is the polarizability tensor of the k-th ion and E_j^k is the j-th component of the total electric field at the k-th ion. Since the induced dipole moments contribute to the electric field themselves, they have been calculated with a self-consistent iterative process. Due to the local symmetry at the sites of the Fe^{3+} and P^{+5} cations and its small ionic radii a significant electric field E^k exists only at the oxygen sites in the $Fe_7(PO_4)_6$ lattice. Thus, only the oxygen ions (α_O) contribute to V_{ij}^{dip}. The α_O value is not well known and was estimated from the best fit of the theoretical EFG's to the measured data. In our calculations, we used values of α_O in the range 0 - 2 $Å^3$. The lattice sums in Eq. (S1) and (S2) were calculated with the spherical boundary method in which the summation is carried out by considering the contributions from all lattice sites inside given radius (r) sphere of 50 Å.

The discrepancy between the calculated and observed EFG values is usually attributed to effects of covalency on the EFG at the nucleus.[S2] One of the main covalent contributions to the EFG tensor (V_{ii}^{ov}) is caused by the overlap of 2s/2p orbitals of the O^{2-} anions with the np orbitals of iron cations:[S3,S4]

$$\begin{aligned} V_{xx}^{\mathrm{ov}} &= -\sum_k^N \tfrac{4}{5}|e|\left(3\sin^2\theta_k \cos^2\varphi_k - 1\right)[\sum_n \left\langle r_{np}^{-3}\right\rangle (S_{np}^k)^2] \\ V_{yy}^{\mathrm{ov}} &= -\sum_k^N \tfrac{4}{5}|e|\left(3\sin^2\theta_k \sin^2\varphi_k - 1\right)[\sum_n \left\langle r_{np}^{-3}\right\rangle (S_{np}^k)^2] , \qquad \text{(S4)} \\ V_{zz}^{\mathrm{ov}} &= -\sum_k^N \tfrac{4}{5}|e|\left(3\cos\theta_k - 1\right)[\sum_n \left\langle r_{np}^{-3}\right\rangle (S_{np}^k)^2] \end{aligned}$$

where the summation over "*k*" extends over all the Fe-O bonds in the (FeO_5)/(FeO_6) polyhedra; $(S_{np}^k)^2 = \{S_{np,s}^2 + S_{np,\sigma}^2 - S_{np,\pi}^2\}$ are the overlap integrals of the *np* orbitals of the iron with the 2*s*/2*p* orbitals of the oxygen O^{2-} ions; θ_k and φ_k are common angular coordinates of the oxygen anion at "*k*" site; $\left\langle r_{nl}^{-3} \right\rangle$ refers to the *nl*-wave function of the Fe^{3+} closed orbitals: $\left\langle r_{3p}^{-3} \right\rangle = 55.93$, and $\left\langle r_{2p}^{-3} \right\rangle = 461.8$ in a.u.[S5] The overlap integrals were calculated using 2*s* and 2*p* Watson's O^{2-} wave functions in a "+3" stabilizing potential and *np* Clementi's wave functions for Fe^{3+}.[S6]

At the final stage, we corrected for shielding effects produced by the own electrons of the iron ions and external charges to obtain the total EFG at the ^{57}Fe nucleus:

$$V_{ij}^{\text{tot}} = (1-\gamma_\infty)V_{ij}^{\text{lat}} + (1-R)V_{ij}^{\text{ov}}, \qquad \text{(S5)}$$

where and γ_∞ = -9.14 and R = 0.32 are Sternheimer factors for these two contributions.[S2] The calculated total contributions to the EFG were diagonalized and the resulting principal values of $\{V_{ii}^{\text{tot}}\}_{i=X,Y,Z}$ were designated according to the usual convention $|V_{ZZ}| \geq |V_{YY}| \geq |V_{XX}|$.

The oxygen dipole polarizability α_O has been estimated with a self-consistent iterative method from the fit of the calculated EFG components to the experimental value of quadrupole splitting. Calculated values for $\boldsymbol{V}^{\text{mon}}$, $\boldsymbol{V}^{\text{dip}}$ and $\boldsymbol{V}^{\text{el}}$ contributions and its dependences as a function of the polarizability of oxygen ions (α_O) in $Fe_7(PO_4)_6$ structure are shown in Fig. S2. The best agreement between the theoretical and experimental values of quadrupole splitting at 300 K was found for the polarizability $\alpha_O \approx 1.7$ Å^3 (for nominal charges Z_O = -2, Z_{Fe} = +2/+3, and Z_P = +5).

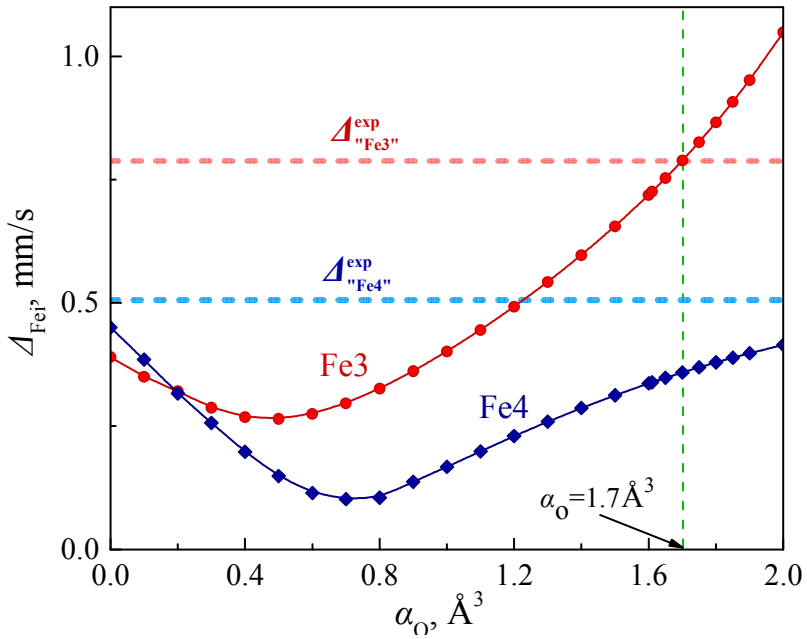

Figure S2. Theoretical dependences of the quadrupole splittings (Δ_{Fei}) as a result of theoretical calculations of total ($\tilde{V}^{tot}$) EFG for two ferrous Fe3 and Fe4 sites (lattice $\tilde{V}^{lat} = (\tilde{V}^{mon} + \tilde{V}^{dip})$ and electronic ($\tilde{V}^{el} \equiv \tilde{V}^{ov}$) contributions versus oxygen polarizability (α_O). The dashed horizontal lines denote the experimental values of the quadrupole splittings Δ_{Fe3} and Δ_{Fe3}. The doted vertical arrow corresponds to the polarizability values $<\alpha_O> \approx 1.7$ Å^3 (*see text*) that allow the best description of the experimental data.

2. *Crystal field calculations.*

The energies (ε_k) of the 3*d* orbitals ($\phi_{p,q}$) for the system are obtained by diagonalizing the real symmetrical matrices:

$$det\left\| H_{pq} - S_{pq}\varepsilon_k \right\| = 0\,, \tag{S6}$$

where $H_{pq} = \left\langle \phi_p \left| \hat{V}_C \right| \phi_q \right\rangle$ and $S_{pq} = \left\langle \phi_p \middle| \phi_q \right\rangle$. We have chosen the real *d* orbitals as a basic set:

$$\begin{aligned}
\psi_1 &= d_{x^2-y^2} = R_{3d}\tfrac{1}{\sqrt{2}}\left[Y_{22} + Y_{22}^*\right],\\
\psi_2 &= d_{xz} = R_{3d}\tfrac{1}{\sqrt{2}}\left[Y_{21} + Y_{21}^*\right],\\
\psi_3 &= d_{z^2} = R_{3d}Y_{20}\,,\\
\psi_4 &= d_{yz} = R_{3d}\tfrac{-i}{\sqrt{2}}\left[Y_{21} - Y_{21}^*\right],\\
\psi_5 &= d_{xy} = R_{3d}\tfrac{-i}{\sqrt{2}}\left[Y_{22} - Y_{22}^*\right],
\end{aligned} \tag{S7}$$

The formal expansion of the crystal potential (V_C) has the form:[S7]

$$V_C = \sum_i^N \frac{Z_i e^2}{r_{ij}} = \sum_i^N Z_i e^2 \left[\sum_{l=0}^{\infty} \sum_{m=-l}^{m=+l} \frac{4\pi}{2l+1} \left(\frac{r_<^l}{r_>^{l+1}} \right) Y_{lm}^*(\theta_i, \varphi_i) Y_{lm}(\theta_i, \varphi_i) \right], \tag{S8}$$

where $Y_{lm}(\theta, \varphi)$ are spherical harmonics describing all angular positions of the *d* electrons, $r_< \equiv r$ and $r_> \equiv R$ are the shorter (electron) and longer (ligands) of the radial vectors connecting the origin to the electron and to ligands (Fig. S3). The H_{pq} integrals are presented in terms of the ligand position functions, D^i_{lm} and G^i_{lm}, listed in Table S1**.** Each D^i_{lm} and G^i_{lm} is characteristic of one ligand and its coordinates, and the sums yielding, $D_{lm} = \sum_i D^i_{lm}$ and $G_{lm} = \sum_i G^i_{lm}$, are taken over all ligands in the (FeO_n) polyhedra. The radial integrals α^i_l in D^i_{lm} and G^i_{lm} are given by

$$\alpha^i_l = Z_i e^2 \int_0^\infty (R_{3d})^2 \left[\frac{r_<^l}{r_>^{l+1}} \right]_i r^2 dr \,, \qquad (9S)$$

In practices the α^i_l integrals and also its ratios $\xi = (\alpha_2/\alpha_4)^i$ frequently are determined experimentally through study of optical absorption spectra in terms of an empirically evaluated parameter such as *Dq*.[S7] In our case, we employ the approximation $\alpha_2 = 4\alpha_4$. The problem reduces thus to evaluation of the H_{pq} integrals and the solution of equations for the five roots ε_k.

For the Fe1 and Fe2 sites the five and six ligands, respectively, affecting the crystal field are assumed identical and of charge *Ze*, with the coordinates enumerated below. The resulting $||H_{pq}||$ matrixes and the numerical evaluation of its H_{pq} elements for Fe1 and Fe2 sites in the local coordinate systems $\hat{o}(x_i,y_i,z_i)$ in $Fe_7(PO_4)_6$ are presented in the Table S3.

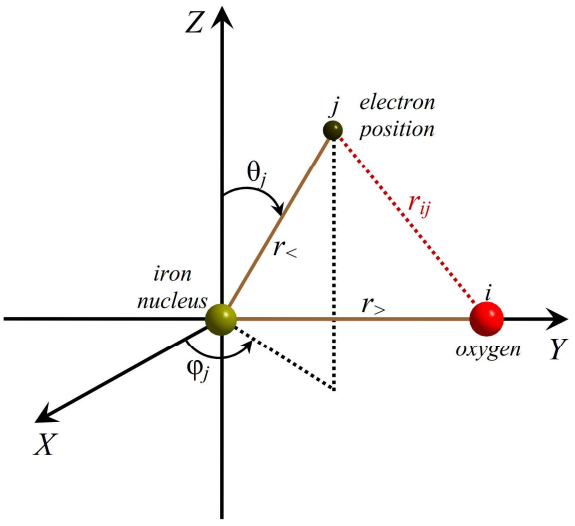

Figure S3. Coordinate system for iron ion and point-charge ligands (oxygen ions).

REFERENCES

(S1) Stadnik, Z. M. Electronic field gradient calculations in rare-earth iron garnets. *J. Phys. Chem. Solids* **1984**, *45*, 311-318.

(S2) *Mössbauer Spectroscopy and Transition Metal Chemistry (Fundamentals and Applications)*; Gütlich, P.; Bill, E.; Trautwein, A. X., Eds.; Springer, Berlin, Heidelberg, 2012.

(S3) Sharma, R. R.; Teng, B. Quadrupole Coupling Constants of Fe^{3+} in Yttrium Iron Garnet. *Phys. Rev. Lett*. **1971**, *27*, 679-681

(S4) Sharma, R. R. Nuclear Quadrupole Interactions in Several Rare-Earth Iron Garnets. *Phys. Rev. B* **1972**, *6*, 4310-4323.

(S5) Watson, R. E. Analytic Hartree-Fock Solutions for $O^{=}$. *Phys. Rev*. **1958**, *111*, 1108-1110.

(S6) Clementi, E. Ab Initio Computations in Atoms and Molecules. *IBM J. Res. Develop*. **1965**, *9*, 2-19.

(S7) Companion, A. L.; Komarynsky, M. A. Crystal Field Splitting Diagrams. *J. Chem. Education* **1964**, *41*, 257-262.

Table S1. The ligand position functions D^i_{lm} and G^i_{lm} (left column), and the integrals H_{pq} in terms of D_{lm} and G_{lm} (right column).

$D^i_{00} = \alpha^i_0$	$H_{11} = D_{00} - \frac{1}{7}D_{20} + \frac{1}{56}D_{40} + \frac{5}{24}D_{44}$
$D^i_{20} = \alpha^i_2\left(3\cos^2\theta_i - 1\right)$	$H_{22} = D_{00} + \frac{1}{14}D_{20} - \frac{1}{14}D_{40} + \frac{3}{14}D_{22} + \frac{5}{42}D_{42}$
$D^i_{40} = \alpha^i_4\left(\frac{35}{3}\cos^4\theta_i - 10\cos^2\theta_i + 1\right)$	$H_{33} = D_{00} + \frac{1}{7}D_{20} + \frac{3}{28}D_{40}$
$D^i_{21} = \alpha^i_2 \sin\theta_i \cos\theta_i \cos\varphi_i$	$H_{44} = D_{00} + \frac{1}{14}D_{20} - \frac{1}{14}D_{40} - \frac{3}{14}D_{22} - \frac{5}{42}D_{42}$
$D^i_{22} = \alpha^i_2 \sin^2\theta_i \cos(2\varphi_i)$	$H_{55} = D_{00} - \frac{1}{7}D_{20} + \frac{1}{56}D_{40} - \frac{5}{24}D_{44}$
$D^i_{41} = \alpha^i_4 \sin\theta_i \cos\theta_i \left(\frac{7}{3}\cos^2\theta_i - 1\right)\cos\varphi_i$	$H_{12} = \frac{3}{7}D_{21} - \frac{5}{28}D_{41} + \frac{5}{12}D_{43}$
$D^i_{42} = \alpha^i_4 \sin^2\theta_i \left(7\cos^2\theta_i - 1\right)\cos(2\varphi_i)$	$H_{13} = -\frac{\sqrt{3}}{7}D_{22} + \frac{5\sqrt{3}}{84}D_{42}$
$D^i_{43} = \alpha^i_4 \sin^3\theta_i \cos\theta_i \cos(3\varphi_i)$	$H_{14} = -\frac{3}{7}G_{21} + \frac{5}{28}G_{41} + \frac{5}{12}G_{43}$
$D^i_{44} = \alpha^i_4 \sin^4\theta_i \cos(4\varphi_i)$	$H_{15} = \frac{5}{24}G_{44}$
$G^i_{21} = \alpha^i_2 \sin\theta_i \cos\theta_i \sin(2\varphi_i)$	$H_{23} = \frac{\sqrt{3}}{7}D_{21} + \frac{5\sqrt{3}}{14}D_{41}$
$G^i_{22} = \alpha^i_2 \sin^2\theta_i \sin(2\varphi_i)$	$H_{24} = \frac{3}{14}G_{22} + \frac{5}{42}G_{42}$
$G^i_{41} = \alpha^i_4 \sin\theta_i \cos\theta_i \left(\frac{7}{3}\cos^2\theta_i - 1\right)\sin\varphi_i$	$H_{25} = \frac{3}{7}G_{21} - \frac{5}{28}G_{41} + \frac{5}{12}G_{43}$
$G^i_{42} = \alpha^i_4 \sin^2\theta_i \left(7\cos^2\theta_i - 1\right)\sin(2\varphi_i)$	$H_{34} = \frac{\sqrt{3}}{7}G_{21} + \frac{5\sqrt{3}}{14}G_{41}$
$G^i_{43} = \alpha^i_4 \sin^3\theta_i \cos\theta_i \sin(3\varphi_i)$	$H_{35} = -\frac{\sqrt{3}}{7}G_{22} + \frac{5\sqrt{3}}{84}G_{42}$
$G^i_{44} = \alpha^i_4 \sin^4\theta_i \sin(4\varphi_i)$	$H_{45} = \frac{3}{7}D_{21} - \frac{5}{28}D_{41} - \frac{5}{12}D_{43}$

Table S2. Angular coordinates of Fe1 and Fe2 oxygen ligands (O*i*).

Fe1			
Ligand	Coordinates		
	θ_i,°	φ_i,°	R_i, Å
O2	90	90	2.016
O8	90	0	2.199
O4	0	0	2.053
O10	90	233.8	1.942
O9	180	0	2.053

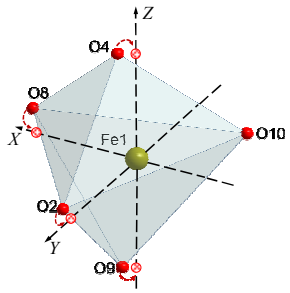

Fe2			
Ligand	Coordinates		
	θ_i,°	φ_i,°	R_i, Å
O1	90	90	2.231
O6	90	0	2.029
O10	0	0	2.311
O1	90	270	2.231
O6	90	180	2.029
O10	180	0	2.311

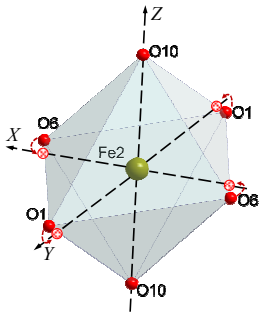

Table S3. The integrals $||H_{pq}||$ matrixes and the numerical evaluation of its H_{pq} elements for Fe1 and Fe2 sites in the local coordinate systems ô(x_i,y_i,z_i) (*see text*).

Fe1 (C_s)

$$\begin{pmatrix} H_{11} & H_{13} & H_{15} & 0 & 0 \\ H_{31} & H_{33} & H_{35} & 0 & 0 \\ H_{51} & H_{53} & H_{55} & 0 & 0 \\ 0 & 0 & 0 & H_{22} & H_{24} \\ 0 & 0 & 0 & H_{42} & H_{44} \end{pmatrix}$$

$$H_{pq} = l \cdot \langle \alpha_0 \rangle + \langle \alpha_4 \rangle \cdot [m \cdot \xi + n]$$

H_{pq}	l	m	n
H_{11}	5.00814	-0.13545	0.30190
H_{22}	5.00814	-0.06068	-0.51019
H_{33}	5.00814	0.13545	0.90535
H_{44}	5.00814	0.19613	-0.69695
H_{55}	5.00814	-0.13545	-0.00011
H_{13}	0	0.14827	0.08087
H_{15}	0	0	-0.15841
H_{24}	0	0.24118	-0.14968
H_{35}	0	-0.27849	-0.12963

Fe2 (D_{2h})

$$\begin{pmatrix} H_{11} & H_{13} & 0 & 0 & 0 \\ H_{31} & H_{33} & 0 & 0 & 0 \\ 0 & 0 & H_{22} & 0 & 0 \\ 0 & 0 & 0 & H_{44} & 0 \\ 0 & 0 & 0 & 0 & H_{55} \end{pmatrix}$$

$$H_{pq} = l \cdot \langle \alpha_0 \rangle + \langle \alpha_4 \rangle \cdot [m \cdot \xi + n]$$

H_{pq}	l	m	n
H_{11}	6.01811	0.14337	1.14861
H_{22}	6.01811	0.06159	-0.76258
H_{33}	6.01811	-0.14337	0.94652
H_{44}	6.01811	-0.20495	-0.49944
H_{55}	6.01811	0.14337	-0.83311
H_{13}	0	-0.15389	-0.11394